ORIGINAL RESEARCH

Analysis of Lung Gene Expression Reveals a Role for Cl^- Channels in Diisocyanate-induced Airway Eosinophilia in a Mouse Model of Asthma Pathology

Adam V. Wisnewski, Jian Liu, and Carrie A. Redlich

Department of Internal Medicine, Yale University School of Medicine, New Haven, Connecticut

Abstract

Diisocyanates are well-recognized causes of asthma. However, sensitized workers frequently lack diisocyanate-specific IgE, which complicates diagnosis and suggests the disease involves IgE-independent mechanisms. We used a mouse model of methylene diphenyl diisocyanate (MDI) asthma to identify biological pathways that may contribute to asthma pathogenesis. MDI sensitization and respiratory tract exposure were performed in Balb/c, transgenic B-cell (e.g., IgE)-deficient mice and a genetic background (C57BL/6)-matched strain. Eosinophils in airway fluid were quantitated by flow cytometry. Lung tissue gene expression was assessed using whole-genome mRNA microarrays. Informatic software was used to identify biological pathways affected by respiratory tract exposure and potential targets for disease intervention. Airway eosinophilia and changes (>1.5-fold; P value < 0.05) in expression of 192 genes occurred in all three mouse strains tested, with enrichment in chemokines and a pattern associated with alternatively activated monocytes/macrophages. CLCA1 (calcium-activated chloride channel regulator 1) was the most upregulated gene transcript (>100-fold) in all exposed mouse lungs versus controls, followed closely by SLC26A4, another transcript involved in Cl^- conductance. Crofelemer, a U.S. Food and Drug Administration–approved Cl^- channel inhibitor, reduced MDI exposure induction of airway eosinophilia, mucus, CLCA1, and other asthma-associated gene transcripts. Expression changes in a core set of genes occurs independent of IgE in a mouse model of chemical-induced airway eosinophilia. In addition to chemokines and alternatively activated monocytes/macrophages, the data suggest a crucial role for Cl^- channels in diisocyanate asthma pathology and as a possible target for intervention.

Keywords: diisocyanate; asthma; chloride; channel; crofelemer

Clinical Relevance

This research provides a model for studying occupational asthma. The data identify changes in lung gene expression that may help decipher pathogenic mechanisms and lead to new ways to treat and prevent disease.

Diisocyanates are widely used throughout the world in polyurethane production, binders, elastomers, and protective coatings (1). Methylene diphenyl diisocyanate (MDI) is the most abundantly produced and utilized diisocyanate, with continually evolving applications (e.g., spray-on truck bed liners, spray polyurethane foam insulation, self-expanding mattresses, three-dimensional printing) (2, 3). The supply and demand of MDI is projected to increase in the foreseeable future (4).

The capacity of diisocyanates to cause asthma was first documented in 1951 by French physicians Fuchs and Valade (5). The clinical presentation, pathology, and natural history of diisocyanate asthma is similar to that caused by environmental allergens and thus theorized to involve an underlying immunologic component and genetic predisposition (6, 7). However, diisocyanate asthma is not associated with well-recognized asthma risk factors (atopy and smoking), and, perhaps more

(Received in original form November 11, 2019; accepted in final form February 25, 2020)

Supported by the Centers for Disease Control through National Institute of Occupational Safety and Health grant OH010941.

Author Contributions: A.V.W., J.L., and C.A.R. each contributed to the design of the work, acquisition of the data, analysis and interpretation of the work, drafting and revising the work, and final approval of the version to be published.

Correspondence and requests for reprints should be addressed to Adam V. Wisnewski, Ph.D., D(ABMLI), Department of Internal Medicine, Yale University School of Medicine, 300 Cedar Street/P.O. Box 208057, New Haven, CT 06520. E-mail: adam.wisnewski@yale.edu.

This article has a data supplement, which is accessible from this issue's table of contents at www.atsjournals.org.

Am J Respir Cell Mol Biol Vol 63, Iss 1, pp 25–35, Jul 2020

Originally Published in Press as DOI: 10.1165/rcmb.2019-0400OC on February 26, 2020
Internet address: www.atsjournals.org

importantly, allergen (e.g., diisocyanate)-specific IgE is not detectable in the majority of affected workers (8, 9). The unusual characteristic of diisocyanate asthma has prompted the hypothesis that its pathogenic mechanisms differ from asthma caused by environmental allergens, which are typically high-molecular-weight compounds (e.g., proteins and pollen) (7, 8, 10, 11).

Deciphering the mechanisms of diisocyanate asthma has been challenging and lags behind models of more common atopic environmental asthma. A major obstacle has been the development of animal models for investigating the genes and pathways central to diisocyanate asthma (12–14). Rodent models, which are readily amenable to transgenic studies, have been challenging to develop, as their distinct upper airway anatomy and its "scrubbing effect" creates a barrier against chemical delivery to the lower airways (15–17). Recently, our laboratory has developed a novel approach for delivering MDI to the lower airways in the form of reversibly reactive glutathione (GSH) conjugates (18). After respiratory tract exposure to GSH-MDI conjugates, MDI can be found bound to the epithelium lining small airways and airway fluid proteins (18, 19). Furthermore, MDI-GSH respiratory tract exposure of immune-sensitized mice, but not naive animals, elicits asthma-like lung pathology, airway eosinophilia, and mucus production (18).

The present study characterizes gene expression changes in the lungs of immune-sensitized mice that receive MDI-GSH via the respiratory tract. Whole-genome mRNA arrays were used to define global changes in gene expression, and informatics was used to identify affected biological pathways. A core set of gene transcripts were associated with MDI-induced airway eosinophilia in multiple mouse strains, including transgenic B-cell–deficient mice, consistent with IgE-independent mechanisms of pathogenesis. The findings suggest a potentially important role for chloride channels, especially CLCA1 (calcium-activated chloride channel protein 1), in response to isocyanate exposure. As CLCA1 regulates the chloride channel, ANO1 (anoctamin 1), the data also suggest a potential pharmacologic target against diisocyanate-induced pathology (20).

The drug crofelemer is one of the most potent inhibitors known for ANO1, providing >90% inhibition, with a half maximal inhibitory concentration (IC_{50}) ~6.5 μM (21). Crofelemer is a purified proanthocyanidin oligomer extracted from the blood-red bark latex of the South American plant *Croton lechleri* (dragon's blood) (21). The sap of *C. lechleri* has been used medicinally for many years in South American countries (22). In the United States, crofelemer is approved by the U.S. Food and Drug Administration for the treatment of noninfectious diarrhea in adult patients with HIV/AIDS on antiretroviral therapy, is taken orally, and does not get absorbed systemically (23). The influence of respiratory tract delivery of crofelemer on the response to MDI in immune-sensitized animals is evaluated as part of the present study.

This study defines global changes in lung gene expression induced by diisocyanate exposure in an animal model of occupational asthma and provides new data connecting lung chloride channels with asthma-like (airway eosinophilia and mucus) responses to chemical exposure. The findings are discussed in the context of diisocyanate occupational asthma pathology and potential targets for pharmacologic intervention. Previously undefined effects of airway chloride channel inhibition on lung gene expression are also discussed.

Methods

Preparation of MDI-GSH Conjugates

Generation and characterization of MDI-GSH reaction products was accomplished as previously described using reduced glutathione and 4,4′-methylenebis(phenyl isocyanate) (CAS No. 101-68-8) from Sigma-Aldrich (18). Control solutions were prepared by adding GSH to MDI that was "mock" reacted in buffer without GSH (during which time MDI hydrolyzes and forms low-molecular-weight ureas incapable of reversibly conjugating GSH) (18, 24). An aliquot of each sample was analyzed by reverse-phase liquid chromatography-coupled mass spectrometry to verify the dominate reaction products between MDI and GSH, as previously described (18, 24).

Skin Sensitization and Airway Exposures of Mice

Eight-week-old male Balb/cJ, C57BL/6J, or B-cell–deficient mice (B6.129S2-$Ighm^{tm1Cgn}$) backcrossed to C57BL/6J were obtained from Jackson Labs, housed under pathogen-free conditions, and fed *ad libitum* with automated water supply under 12-hour day/night light cycles. Immunologic sensitization to MDI via skin exposure and subsequent respiratory tract exposure to MDI-GSH conjugates were performed as previously described (18, 25). All studies followed guidelines established in the Guide for the Care and Use of Laboratory Animals prepared by the Institute of Laboratory Animal Resources, National Research Council (26) and were approved by Yale's Institutional Animal Care and Use Committee.

Crofelemer Preparation and Treatment

Mytesi tablets from Napo Pharmaceuticals were solubilized as previously described (27). The concentration of the final solution was calculated based on the extinction coefficient of crofelemer of 7.6 ml/(mg cm) at 280 nm (27). In some studies, 4 hours before MDI exposure, mice received either mock exposure (ultrapure water) or the murine equivalent of the recommended human daily dose (~4 mg/kg) of Mytesi (28) via intranasal administration under light anesthesia (isoflurane) of 50 μl of a 1.6 mg/ml crofelemer solution.

BAL Analysis and Lung Tissue RNA Purification

BAL and lung tissue samples were obtained 48 hours after the last respiratory tract exposure and processed as previously described (18, 25). Flow cytometry analysis of BAL cells for eosinophils was accomplished using the protocol defined by Stevens and colleagues. (29). Perfused lung tissue was obtained for histology, and RNA was purified using an RNeasy kit from Qiagen according to the manufacturer's recommendations.

Lung Gene Expression (Microarray) Analyses

Processing of RNA and microarray analyses were performed by the Yale Center for Genome Analysis as described online (30, 31). All reactions and hybridizations were performed using Affymetrix Mouse Clariom-S arrays according to the manufacturer's protocol. Data analysis and software are described in the METHODS section of the data supplement. Complete microarray data are available in the Gene Expression Omnibus (GEO) database (accession number: GSE136146).

Real-Time PCR Studies

Bio-Rad's PrimePCR SYBR Green Assay for CLCA1 aka murine CLCA3 (qMmuCID0009928) and ACTB (qMmuCED0027505) were used according to manufacturer's directions, with cDNA prepared using an iScript cDNA synthesis kit (Bio-Rad).

Statistical Analyses

Significance of differences in BAL cell numbers, real-time PCR data, and microarray fluorescence values were determined based on ANOVA. False discovery rate (FDR) *P* values for microarrays were calculated using the approach of Benjamini (32).

Results

Airway Eosinophilia in a Mouse Model of MDI Asthma

We initially measured airway eosinophilia in a mouse model of MDI asthma, in which chemical is delivered to the respiratory tract as reversibly reactive GSH conjugates (18). Eosinophils in the BAL were quantitated by flow cytometry on the basis of their expression of $CD45^+$, $CD11B^+$, Siglec-F^+, and $CD11C^{lo}$, as Stevens and colleagues describe (29). BAL from MDI-sensitized and exposed Balb/c mice contained significantly ($P < 0.05$) increased numbers of eosinophils versus controls, as we have previously reported (Figure 1) (18). Moreover, respiratory tract MDI exposure induced airway eosinophilia in B-cell–deficient transgenic mice, as well as C57BL/6, the genetic background for the B-cell–deficient mice (Figure 1). Histology analysis further demonstrated lung tissue eosinophilia and substantial airway mucus in MDI-sensitized/exposed B-cell–deficient mice (*see* Figure E1 in the data supplement). The data are consistent with clinical findings of diisocyanate asthma without chemical-specific IgE, which can only be produced by B cells (33).

Core Changes in Lung Tissue Gene Expression in a Mouse Model of MDI Asthma

Lung gene expression in our mouse model of MDI asthma was initially analyzed using principal component analysis and Venn diagrams. By principal component analysis (Figure 2), MDI and control mice were readily differentiated, as were differences between species. In Balb/c mice, 551 gene transcripts were differentially expressed (>1.5-fold change fluorescence; $P < 0.05$) in MDI-exposed versus control mice. In C57BL/6 mice, 602 gene transcripts, and in B cell deficient mice 1,385 gene transcripts, were differentially expressed in MDI-exposed versus control mice. At the core of the molecular changes that MDI respiratory tract exposure causes in sensitized hosts (vs. control mice) from all three mouse strains tested, were 192 differentially expressed transcripts; 163 consistently increased and 29 consistently decreased (GEO data set accession number GSE136146).

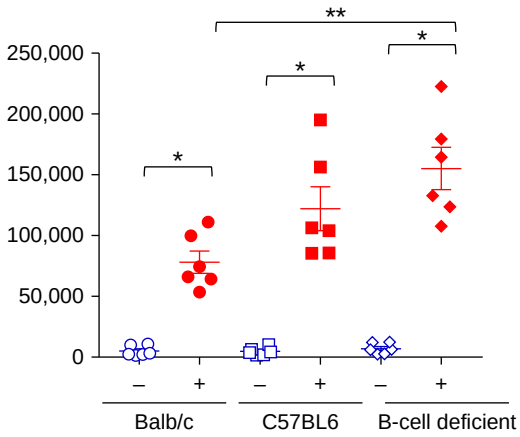

Figure 1. Airway eosinophilia induced by respiratory tract exposure to methylene diphenyl diisocyanate (MDI). The number of eosinophils collected by BAL (*y*-axis) from MDI-sensitized mice from different genetic backgrounds exposed to MDI (+) or control (−). The figure shows the mean ± SEM from one of three representative experiments with $n = 6$ mice/group. $^*P < 0.001$ and $^{**}P < 0.05$ by ANOVA.

Lung Tissue Gene Transcripts with Largest Changes in a Mouse Model of MDI Asthma

Volcano plots (Figure 3) of the microarray data readily identify CLCA1 as the gene transcript with the greatest relative increase in MDI-exposed versus control animals of all three mouse strains tested. CLCA1 had previously been identified as the most upregulated protein in BAL fluid from sensitized/exposed Balb/c mice in the present MDI asthma model (18). A second Cl^- conductance-related gene transcript, the solute carrier family 26, member 4 (SLC26A4 aka pendrin), was the eighth most increased transcript in Balb/c mice, the second most increased transcript in C57BL/6, and the third most increased transcript in B-cell–deficient mice exposed to MDI versus control mice.

The 10 core transcripts most increased in MDI-exposed mice versus control mice (among the top 8 in each mouse strain tested) and the 5 transcripts most consistently decreased are listed in Table 1. The genes encoding many of these transcripts have well-established associations with asthma, airway eosinophilia, and mucus in human patients and/or experimental animal models of asthma or cytokine-induced airway inflammation (20, 34–38). The proteins corresponding to eight gene transcripts (CLCA1, CHIL4, CHITL3, RETNLA, FCGBP, C1QB, PIGR, and CTSS) were significantly ($P < 0.05$) increased in BAL fluid in prior proteomic studies of the current MDI asthma model in Balb/c mice (18).

Grouping/Classification of Lung Tissue Genes Differentially Expressed in a Mouse Model of MDI Asthma

More than half of 92 transcripts increased more than twofold in MDI-sensitized and -exposed versus control mice can be grouped into functional categories, as shown in the cluster analysis in Figure 4. These include transport proteins (CLCA1, SLC26A4, SLC5A1 SLC7A8, and ATPV06D2), chemokines (CCL6, CCL8, CCL9, CCL11, CCL12, CCL17, and CCL22), complement proteins (C1QA, C1QB, C1QC, C3, C3AR1, and CFB), Ig-F_c related proteins (FCGBP, FCGR2B, FCGR3, and PIGR), CD20-like proteins, growth factors, nuclear factors, and numerous genes related to monocyte/dendritic cell maturation, alternatively activated macrophages, and related innate immune responses including

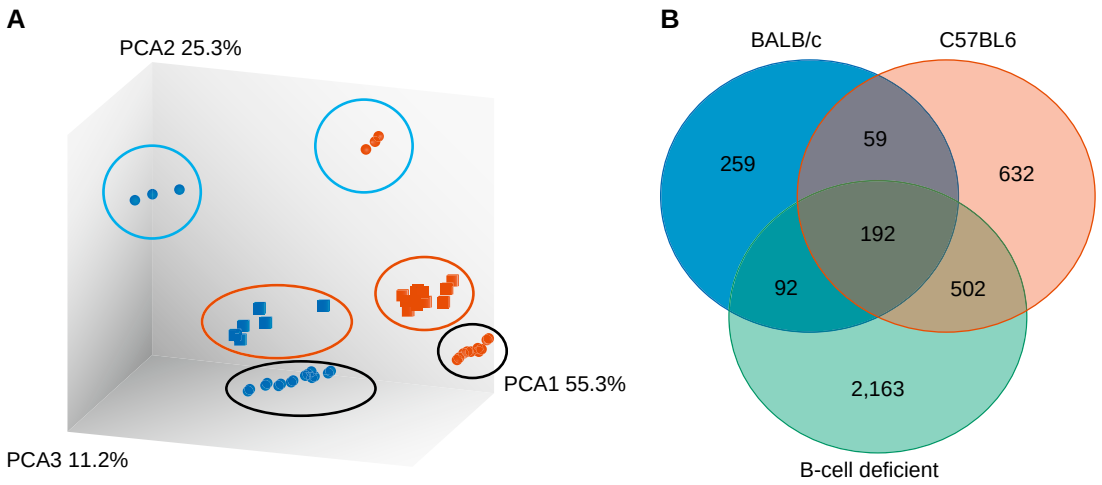

Figure 2. Principal component analysis (PCA) and Venn diagram visualization of microarray data. Lung gene expression affected by MDI respiratory tract exposure was evaluated in different mouse strains. (*A*) In the PCA, Balb/c mice are circles, C57BL/6 mice are squares, and B-cell–deficient mice are circled in black; blue are control exposed and red are MDI exposed. (*B*) In the Venn diagram, the subset of lung tissue genes differentially expressed (>1.5-fold; $P < 0.05$) in MDI versus control exposed hosts are depicted for Balb/c, C57BL/6, and B-cell–deficient mice. Genes differentially expressed in all three strains are identified by the overlapping core. Data include $n = 3$ control Balb/c, $n = 3$ MDI-exposed Balb/c, $n = 6$ control C57BL/6, $n = 14$ MDI-exposed C57BL/6, $n = 9$ control B-cell–deficient, and $n = 7$ MDI-exposed B-cell–deficient mice.

CLEC7A (Dectin1), CD209E (DC-SIGN), LY86, MGL2, and chitinases (CHIA, CHIL3, CHIL4, aka AMCASE, YM1, and YM2) (39).

Mouse Strain Differences in Lung Tissue Gene Expression in a Mouse Model of MDI Asthma

Limited strain differences were noted in the MDI response between Balb/c, C57BL/6, and B-cell–deficient mice (Figures E2–E4). HAL (histidine ammonia lyase) was increased in MDI versus control (5.8-fold; FDR P value $< 10^{-6}$) exposed Balb/c mice, but not C57BL/6 or B-cell–deficient mice. In contrast, phospholipase A2 group IVC (PLA2G4C) was increased in MDI versus control (more than ninefold; FDR P value $< 10^{-4}$) exposed C57BL/6 and B-cell–deficient mice, but not Balb/c mice. B-cell–deficient mice, compared with C57BL/6 and Balb/c mice, exhibited higher expression levels of uncharacterized genes Gm3893, Gm10600, and TMEM254 and lower levels of CD19, CD79A, and J-chain transcripts (as expected). In addition, strain differences between Balb/c and C57BL/6 lung expression of TRIM30D, APOBEC3, and PYDC4 were noted under all conditions (Figure E4).

Bioinformatic Analyses of Lung Tissue Gene Expression in a Mouse Model of MDI Asthma

Two different bioinformatic software programs were used to analyze the biological pathways and networks associated with the MDI-induced gene expression changes. Transcriptome Analysis Console identified chemokines as the most significantly affected pathway, with seven upregulated genes and no downregulated genes. Ingenuity Pathway Analysis associated the gene expression data with five canonical pathways: granulocyte adhesion and diapedesis, agranulocyte adhesion and diapedesis, atherosclerosis signaling, phagosome formation, and complement system. The top network is shown in Figure E5 and includes 19 focus molecules related to cell-to-cell signaling/interaction, hematological, and immunologic disease. Analysis matching of the lung gene expression data demonstrated closest similarity with GEO data set GSE35979 on IL-13–induced mouse lung inflammation. Perhaps most notably, Ingenuity Pathway Analysis identified crofelemer as the only drug to target CLCA1, the transcript most increased in the lungs of MDI-sensitized/exposed mice versus control mice (Figure E6).

Effect of Crofelemer on Isocyanate Exposure-induced Changes in Immune Sensitized Mice

Crofelemer in ultrapure water was delivered intranasally at the murine equivalent of the recommended human daily dose (on a mg/kg basis) 4 hours before MDI exposure, as described in the Methods section. Gene expression, airway eosinophilia, and mucus levels were subsequently assessed in mice exposed to MDI, MDI + crofelemer, or crofelemer alone versus control animals.

Crofelemer pretreatment significantly reduced lung tissue CLCA1 transcript levels in MDI-sensitized/exposed mice (as well as control mice), as shown in the volcano plots and bar graphs in Figure 5. In MDI-sensitized/exposed mice, crofelemer also reduced expression of other top transcripts (defined in Table 1) increased in MDI versus control mice. Of note, lung tissue from mice given crofelemer alone (vs. "mock"-treated control mice) exhibited numerous changes in histone cluster 1 and 2 gene transcripts, also highlighted in the volcano plot in Figure 5A.

Effect of Crofelemer on Isocyanate Exposure-induced Airway Eosinophilia and Mucus

Along with changes in gene transcription, crofelemer abrogated MDI-induced airway eosinophilia as measured by flow cytometry. As shown in Figure 6, BAL from mice treated with crofelemer before MDI exposure contained significantly ($P < 0.05$) reduced levels of eosinophils versus mice exposed to MDI without crofelemer pretreatment, indistinguishable from that of control mice treated with crofelemer alone.

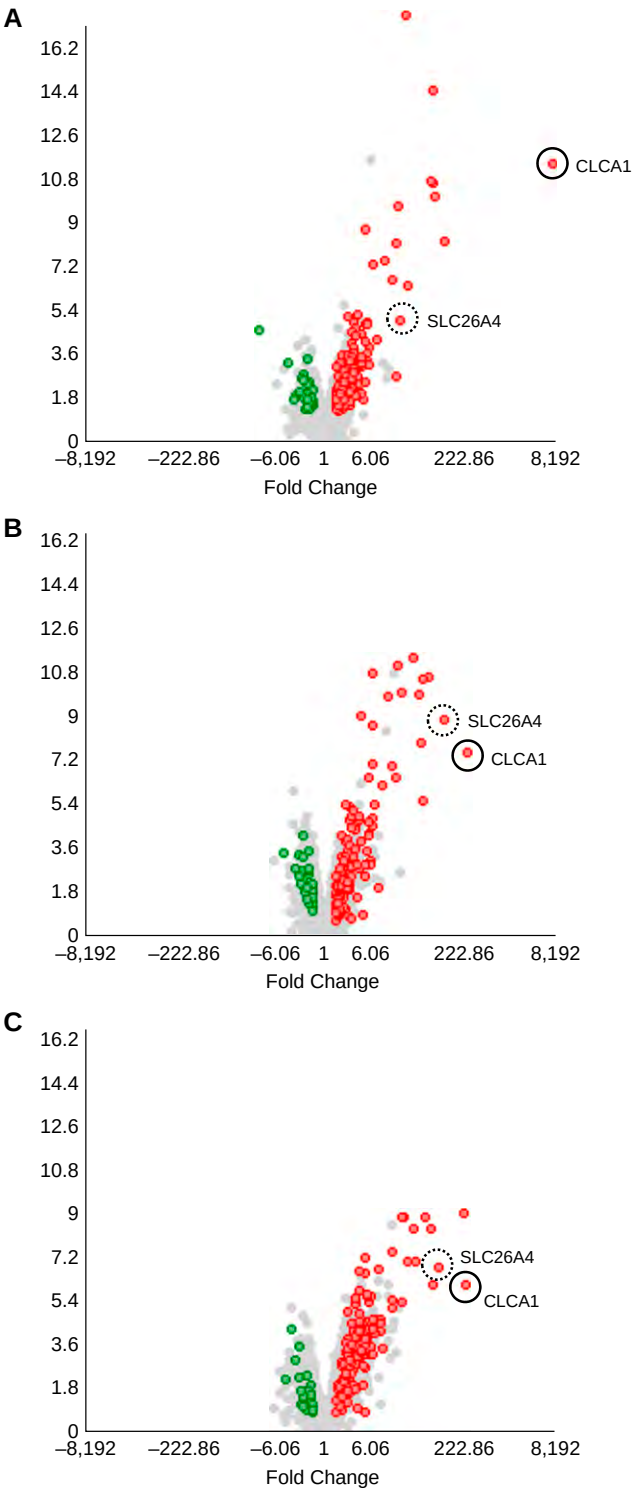

Figure 3. Volcano plots of microarray data. Lung tissue whole-genome mRNA microarray data of MDI-sensitized mice exposed to MDI (glutathione conjugates) versus control are shown for (*A*) Balb/c, (*B*) C57BL/6, and (*C*) B-cell–deficient mice. Fold change is expressed on the *x*-axis and false discovery rate *P* value is expressed on the *y*-axis. The gene transcript (CLCA1) most increased in MDI-exposed versus control mice is highlighted, along with a second Cl^- conductance–related gene (SLC26A4). Data include $n = 3$ control Balb/c, $n = 3$ MDI-exposed Balb/c, $n = 6$ control C57BL/6, $n = 14$ MDI-exposed C57BL/6, $n = 9$ control B-cell–deficient, and $n = 7$ MDI-exposed B-cell–deficient mice. CLCA1 = chloride channel accessory 1; SLC26A4 = solute carrier family 26 member 4.

Pretreatment of mice with crofelemer also abrogated MDI induction of airway mucus based on periodic acid-Schiff staining of lung tissue sections (Figure 7). Although MDI-sensitized/exposed C57BL/6 mice developed increased airway mucus (and associated tissue eosinophilia), mice pretreated with crofelemer before MDI exposure (or exposed to crofelemer alone) failed to develop similar pathology.

Together, gene expression, flow cytometry, and histology data from *in vivo* studies support the hypothesis that CLCA1 (possibly acting through ANO1, the channel it regulates) plays an important role in diisocyanate exposure–induced asthma-like airway inflammation.

Validation of Microarray Data for CLCA1

Real-time quantitative PCR was performed for the gene (CLCA1) most increased in sensitized MDI-exposed versus control mice. Changes in CLCA1 expression were calculated based on the ΔΔCt approach, with β-actin (ACTB) as a reference gene (40). Analysis of RNA samples from replicate animals in each exposure group were consistent with microarray data and confirmed increased CLCA1 transcript levels in MDI-sensitized/exposed mice (vs. control mice) and diminution of this response in crofelemer-treated mice (Figure E7). Real-time quantitative PCR analysis also validated microarray-defined decreases in baseline CLCA1 expression in control mice treated with crofelemer (Figure E7).

Discussion

This study focuses on molecular changes associated with MDI-induced airway eosinophilia using a mouse model of MDI asthma in which chemical is delivered to the lower airways as reversibly reactive GSH conjugates. Studies were performed in multiple mouse strains, including B-cell–deficient mice, given the frequent lack of "antigen-specific" IgE in hypersensitized individuals and the possibility that diisocyanate allergy/asthma occurs via IgE-independent mechanisms (33). The data identify a core set of 192 gene transcripts associated with MDI-induced airway eosinophilia in all sensitized mouse strains tested, including B-cell–deficient mice. Gene expression

Table 1. Lung Tissue Gene Transcripts Most Affected in Mouse Model of Methylene Diphenyl Diisocyanate Asthma Pathology

Gene Symbol	Gene Name	BALB/c Fold Change	C57BL/6 Fold Change	B Cell$^{-/-}$ Fold Change
CLCA1	Chloride channel accessory 1	5,820 (9.6×10^{-13})	228 (2.1×10^{-11})	214 (8.9×10^{-7})
SLC26A4	Solute carrier family 26, member 4, pendrin	18 (1.2×10^{-2})	95 (6.0×10^{-13})	74 (1.7×10^{-7})
MUC5AC	Mucin 5, subtypes A and C, tracheobronchial/gastric	58 (6.2×10^{-7})	54 (2.4×10^{-11})	56 (4.8×10^{-9})
MMP12	Matrix metallopeptidase 12	3.9 (0.93)	42 (3.1×10^{-9})	60 (1.0×10^{-6})
RETNLA	Resistin-like alpha	57 (2×10^{-6})	41 (2.9×10^{-11})	45 (1.6×10^{-9})
RNASE2A	RNase, RNase A family, 2A (liver, eosinophil-derived neurotoxin)	95 (3.1×10^{-6})	39 (1.2×10^{-8})	194 (1.2×10^{-9})
CCL8	Chemokine (C-C motif) ligand 8 (MCP2)	66 (4.5×10^{-7})	38 (1.2×10^{-10})	31 (1.3×10^{-7})
FCGBP	Fc fragment of IgG binding protein	16.6 (9.2×10^{-7})	29 (3.9×10^{-12})	20 (1.6×10^{-9})
CHIA	Chitinase, acidic 1 (AMCase)	7.3 (0.23)	19 (9.9×10^{-11})	29 (5.0×10^{-9})
CHIL4	Chitinase-like 4 (YM-2)	62 (1.1×10^{-8})	12 (1.4×10^{-10})	13 (4.1×10^{-8})
PON1	Paraoxonase 1	−4.1 (0.59)	−4.8 (0.0004)	−4.4 (0.0067)
DUSP1	Dual specificity phosphatase 1	−3.4 (0.99)	−2.54 (0.0036)	−2.43 (0.023)
DUSP8	Dual specificity phosphatase 8	−2.9 (0.93)	−2.4 (0.0031)	−2.0 (0.14)
ADAMTS1	A disintegrin-like and metallopeptidase with thrombospondin type 1 motif, 1	−2.5 (0.43)	−1.8 (0.0029)	−2.19 (0.0378)
NR4A1	Nuclear receptor subfamily 4, group A, member 1, Nur77	−12.1 (0.017)	−3.1 (0.0016)	−2.4 (0.079)

Data are shown as false discovery rate (*P* value).

patterns for myeloid lineage, including innate cells and alternatively activated macrophages, were markedly increased in MDI-exposed mice, consistent with prior BAL proteomic studies using the present mouse model and *in vitro* studies with human blood cells (10, 18, 41). The data also identify significant MDI-induced changes in transport molecules, with the greatest relative change in CLCA1, a gene previously associated with human asthma and known to regulate the chloride channel ANO1 (20). Experimental treatment of mice with a potent ANO1 inhibitor, crofelemer (23), limited MDI-associated increases in CLCA1 (and other top MDI-induced genes) transcripts and abrogated airway eosinophilia and mucus. Together, the data suggest a role for Cl^- channels in diisocyanate asthma pathology and as possible targets for pharmacologic intervention.

The present CLCA1 gene expression data are consistent with our recent mass spectrometry–based identification of CLCA1 as the most upregulated protein in airway fluid of MDI-sensitized and -exposed mice (18). Increases in CLCA1 transcripts have been observed in other mouse models of allergic and T-helper cell type 2 cytokine-driven airway inflammation, and genetic polymorphism has been associated with human asthma (18, 35, 37, 42, 43). Woodruff and colleagues identified CLCA1 as the most upregulated transcript in epithelial cells from human patients with asthma versus healthy control subjects (35). CLCA1 expression is believed to play an important role in asthma pathogenesis by serving as the master regulator of IL-13 to mucin gene expression signaling (44). The ability of diisocyanate to induce CLCA1 is remarkable, given the noted lack of T-helper cell type 2 T-cell (e.g., IL-4, IL-13) and associated antigen-specific IgE responses among patients with isocyanate asthma (7, 9, 10, 33, 45).

Another apical airway Cl^- channel gene associated with asthma, SCL26A4 (aka Pendrin) (46), was also among the gene transcripts most increased in mice exposed to MDI via the respiratory tract versus control mice. MDI exposure–associated changes in Cl^- channel transcripts are consistent with the chemical's induction of mucus observed histologically in sensitized mice and workers and the well-established importance of chloride secretion to airway mucus levels (7, 18, 47). A role for Cl^- channels in asthma has been recognized previously, and certain inhibitors, (e.g., niflumic acid) have been shown to suppress airway inflammation (48). In the present study, crofelemer, a more potent and specific Cl^- channel inhibitor than niflumic acid (IC_{50} 6.5 vs. 26.5 μM for ANO1 channel) (21, 48), suppressed MDI-induced asthma-like pathology, further suggesting an important contribution of airway Cl^- conductance to asthma (21).

The possibility that crofelemer might be used in the treatment of asthma should be considered with caution, as potential adverse health effects from respiratory dosing will require investigation beyond the scope of this study. The present microarray data suggest that intranasal delivery of crofelemer causes significant gene expression increases in histone cluster 1 genes, tenascin C, NADH dehydrogenase subunit 6, and numerous uncharacterized murine genes (Figure 5A and not shown). Some crofelemer-treated mouse lungs also contained localized pockets of tissue inflammation resembling monocytic pneumonia. Future investigation will better define the health effects of crofelemer delivery to the lower respiratory tract, including potential toxic as well as therapeutic responses.

Bioinformatic analyses of differential gene expression in our MDI-asthma model noted marked overlap with prior published animal models of asthma (GSE35979) as well as clinical investigations. A prominent similarity was MDI's induction of chemokine genes and the predicted canonical pathway for granulocyte adhesion and diapedesis in all animals tested, including B-cell–deficient mice.

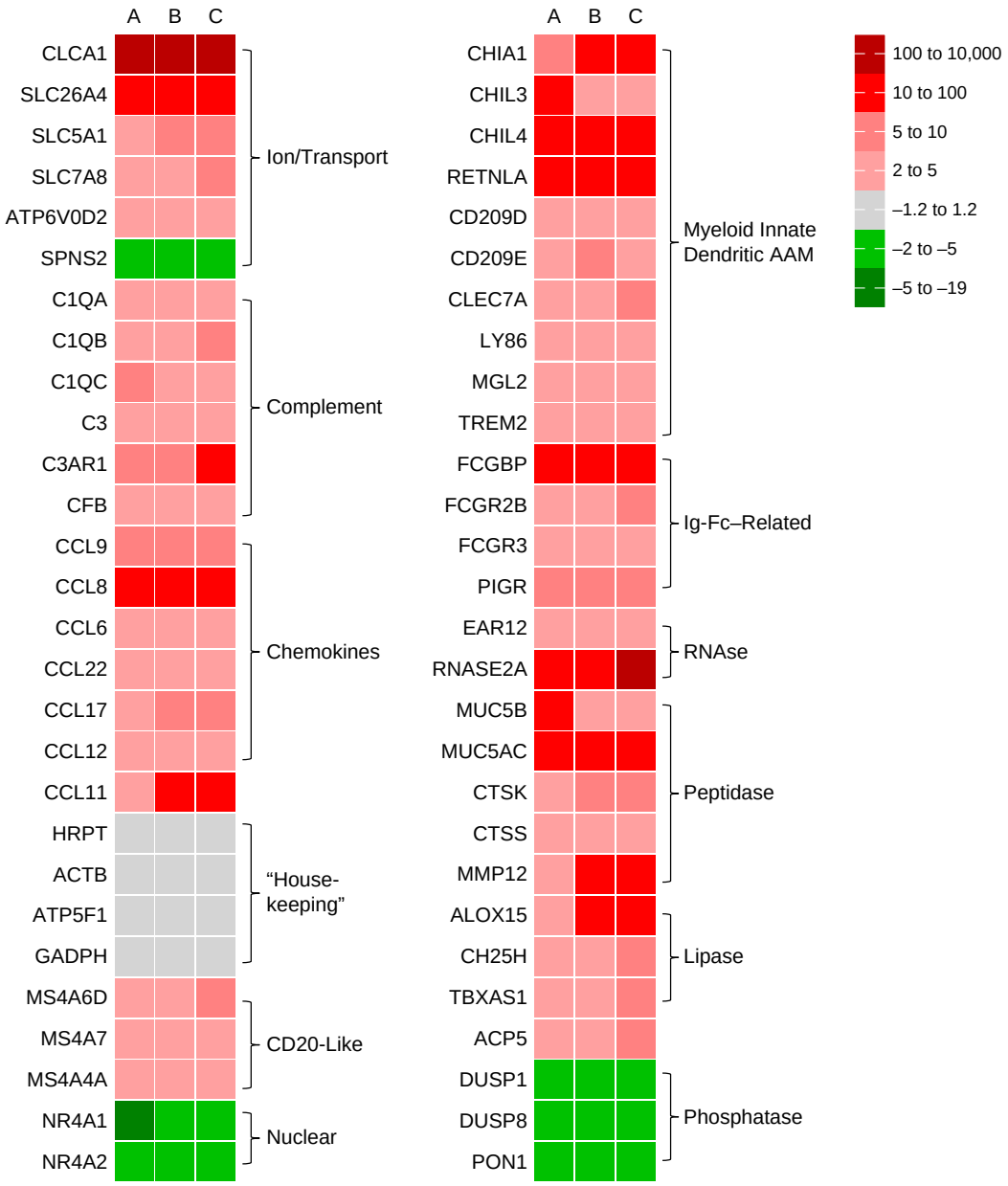

Figure 4. Categorization of differentially expressed genes in lungs of MDI-sensitized/exposed mice. A heat map of microarray data from MDI versus control mouse lung tissue is provided for studies described in Figures 2 and 3, with three different mouse strains: Balb/c (A), C57BL/6 (B), and B-cell–deficient (C) mice. Genes are grouped according to known function/association using bioinformatic software and published literature. AAM = alternatively activated macrophages.

The present chemokine gene expression data are consistent with the pathology observed in our MDI-asthma mouse model as well as human disease, where patients' MDI-induced blood cell chemokine production associates with chemical sensitivity better than their antigen-specific serum IgE (10). In the present study, relatively high levels of CCL11 (eotaxin) transcript explain the marked eosinophilia in MDI-sensitized/exposed hosts, whereas relative increases in CCL12 transcript (the mouse chemokine with greatest homology to human MCP-1) are consistent with the association of isocyanate asthma with "antigen"-induced blood cell MCP-1 production *in vitro* (10). The mechanism through which MDI exposure induces chemokine production is likely an important aspect of pathogenesis that remains poorly understood.

The present gene expression data are consistent with prior studies noting the ability of isocyanates to induce myeloid/innate immune responses and alternatively activated macrophages *in vitro* and *in vivo* (18, 41). Specific gene transcripts CHIL3, CHIL4 (YM1, YM2), RETNLA (RELMA, FIZZ1), CLEC7A

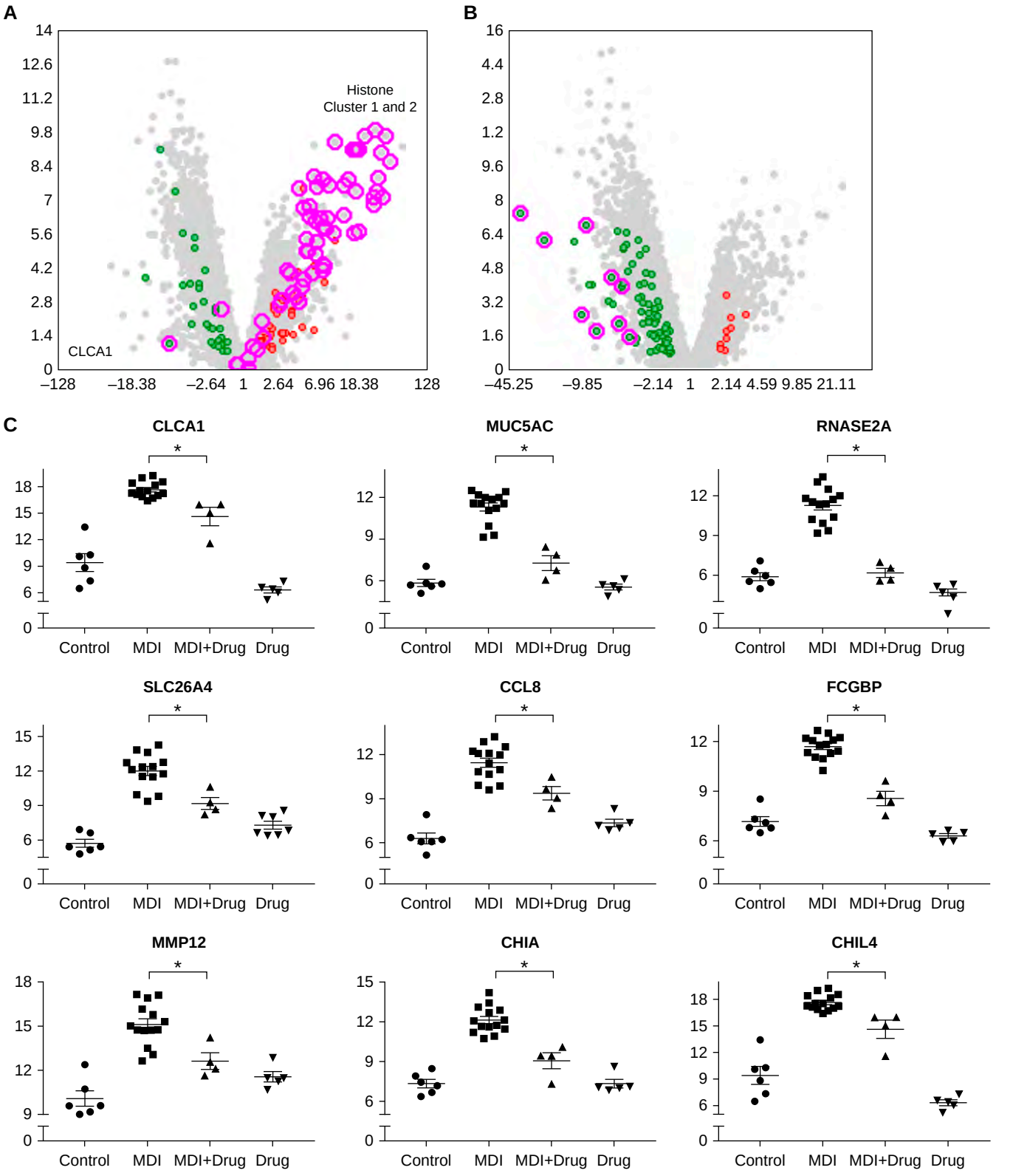

Figure 5. Effects of crofelemer on lung gene expression in MDI-sensitized/exposed mice. Volcano plot *x*-axis depicts fold change, and the *y*-axis depicts false discovery rate *P* value for individual lung genes in (*A*) $n = 5$ mice treated with crofelemer versus $n = 6$ untreated control mice, and (*B*) $n = 4$ mice pretreated with crofelemer before MDI exposure versus $n = 14$ mice exposed to MDI without crofelemer. The 192 differentially expressed MDI gene transcripts that are also 1.5-fold differentially expressed under conditions ± crofelemer are solid colored (red/green). Circled in pink are (*A*) histone cluster

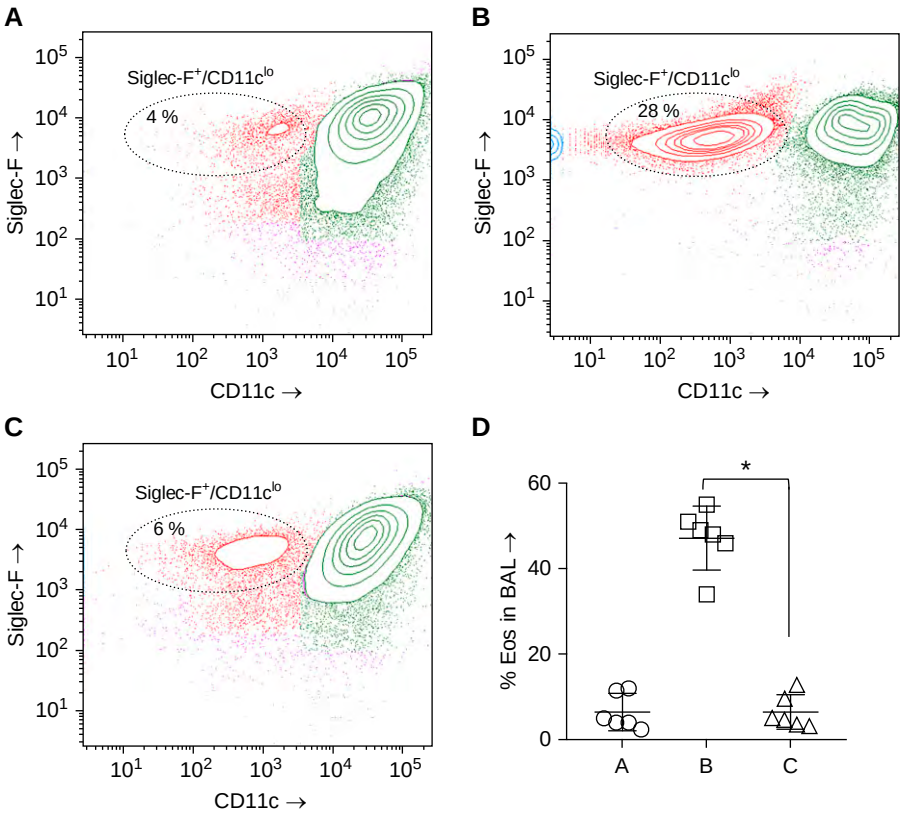

Figure 6. Effect of crofelemer on airway eosinophilia in MDI-sensitized/exposed hosts. Eosinophils in the BAL ($CD11c^{lo}$, Siglec-F^{+}) are highlighted in flow cytometry contour plots of BAL cells from (*A*) representative MDI-sensitized mice exposed to crofelemer alone, (*B*) respiratory tract MDI, or (*C*) crofelemer + respiratory tract MDI. All data are gated on single $CD45^{+}$ live cells. (*D*) Mean ± SEM of percentage eosinophils (Eos) (*y*-axis) from one of three experiments with $n = 6$ mice each, demonstrating a significant (*$P < 0.05$) difference in MDI-exposed mice with and without crofelemer pretreatment (groups C and B, respectively). Siglec-F = sialic acid–binding immunoglobulin-like lectin F.

(Dectin1), CLEC10A (MGL2), and CD209E (DC-SIGN) are considered markers for alternatively activated macrophages (39, 49) and are among the transcripts most strikingly increased in MDI-exposed (vs. control) mice in each of the genetic strains tested herein. However, the mechanism through which isocyanates induce alternative macrophage activation remains puzzling, as this process is believed to involve cytokines (IL4/IL13) generally not associated with human isocyanate asthma (7, 9, 10, 33). A search of available gene expression data (e.g., GEO) from human lung that might be compared with the present data was unsuccessful. However, an early microarray study (with a 4K gene chip) of human peripheral blood cells exposed to hexamethylene diisocyanate also noted increases in chitinases, lysosomal ATPase, and ACP5 consistent with stimulation of monocyte/macrophage lineages (41).

The present gene expression data highlight differences in lung gene expression between different mouse strains both in response to MDI and in control animals. The most substantial differences were noted in HAL and PLA2G4C, which were differentially expressed in response to MDI in Balb/c versus C57BL/6 mice. The data also identified MDI-induced expression of several uncharacterized murine gene transcripts with similarity to each other, and limited homology (<50%) with human FAM205A2 in B-cell–deficient mice versus C57BL/6 wild-type mice. The impact of strain differences in MDI exposure responses to the development of MDI asthma remains unknown but could be relevant to individual differences in sensitivity noted among workers with similar exposures (50).

The strengths and weaknesses of the present study are important to recognize when considering the findings' clinical relevance. The strengths include the well-controlled animal model (including hosts lacking B cells/IgE), whole-genome expression assessment, bioinformatic-guided discovery experiments, and real-time PCR validation of microarray findings on CLCA1 expression. The major weaknesses include translational unknowns inherent to all animal models of human disease and the use of reversibly reactive GSH conjugates to achieve lower airway MDI exposure, possibly bypassing unrecognized *in vivo* reactions. As with all microarray data, the possibility of batch effects due to technical issues cannot be ruled out. In addition, it should be recognized that crofelemer is not entirely specific for ANO1 and also inhibits the CFTR (cystic fibrosis transmembrane conductance regulator) with a similar IC_{50} (~7 μM) but to a lesser extent (<60% for CFTR vs. >90% for ANO1) (21). Future studies should clarify the relevance of the present animal model to occupational asthma caused by diisocyanate exposure and the extent to which airway Cl^{-} conductance is involved.

In summary, we used an animal model of MDI-induced airway eosinophilia to characterize changes in lung gene expression after respiratory tract exposure of sensitized hosts. Studies were performed in multiple mouse strains (including

Figure 5. (*Continued*). genes and (*B*) genes most increased in MDI versus control exposed lung tissue. (*C*) Mean ± SEM of microarray fluorescence signals (log_2) for genes of interest (as labeled) in MDI-sensitized/exposed mice ± crofelemer (drug) pretreatment versus control mice, with and without crofelemer treatment as labeled. *Indicates $P < 0.05$ between groups. Studies were performed with $n = 6$ control, $n = 14$ MDI, $n = 4$ MDI + crofelemer, and $n = 5$ crofelemer-only treated C57BL/6 mice. CHIA = chitinase acidic; CHIL4 = chitinase-like 4; FCGBP = Fc fragment of IgG binding protein; MMP12 = matrix metallopeptidase 12; MUC5AC = mucin 5AC; RNASE2A = ribonuclease RNase A family member 2A.

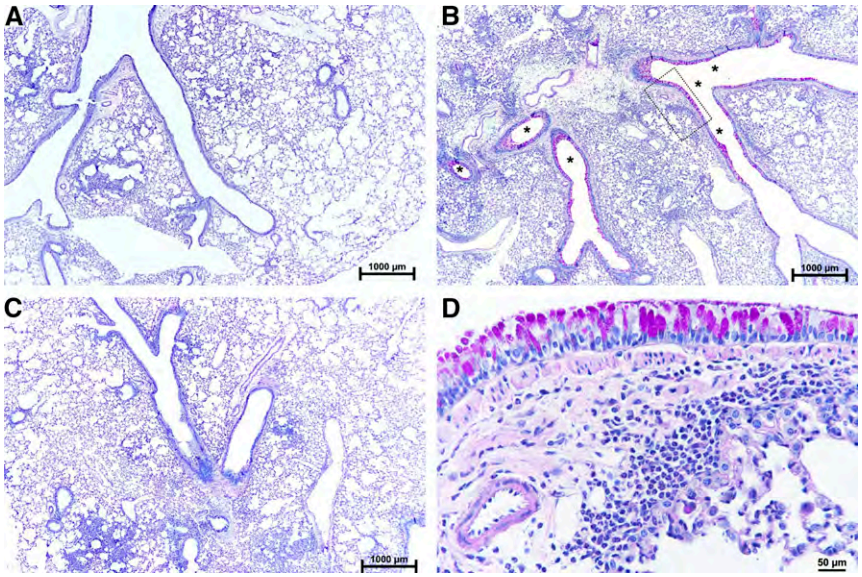

Figure 7. Effect of crofelemer on airway mucus in MDI-sensitized/exposed hosts. Periodic acid–Schiff–stained lung tissue sections from (*A*) MDI-sensitized mice exposed to crofelemer alone, (*B*) respiratory tract MDI, or (*C*) crofelemer + respiratory tract MDI. The asterisks in *B* highlight airways lined with mucus-producing cells. (*D*) The area outlined in *B* under higher magnification to highlight mucus-producing cells lining the airway and eosinophils in the underlying tissue. Representative data are from one of three experiments with $n = 3$ mice each. Scale bars: *A–C*, 1,000 μm; *D*, 50 μm.

B-cell–deficient mice) to identify lung gene expression changes (including those that might be IgE independent) at the core of MDI-induced pathology. Genome-wide profiling defined 192 differentially expressed genes in all MDI-sensitized/exposed mice versus control mice, dominated by relative increases in transcripts for CLCA1, other transport proteins, and markers of myeloid differentiation (e.g., innate cells and alternatively activated macrophages). Respiratory tract dosing of mice with crofelemer (an inhibitor of ANO1, the Cl^- channel regulated by CLCA1) before exposure to MDI reduced chemical-induced changes in expression of key asthma genes, airway eosinophilia, and mucus levels. Together, the data provide a model for IgE-independent asthma-like pathology in response to diisocyanate exposure and accumulating evidence of an important role for alternatively activated macrophages. The data also suggest that exposure-induced CLCA1 and/or Cl^- conductance plays an important role in diisocyanate-induced pathology and may be a target for disease intervention. ■

Author disclosures are available with the text of this article at www.atsjournals.org.

Acknowledgment: The authors thank Sok Meng (Evelyn) Ng from the Yale West Campus Center for Genome Analysis for expert technical performance of RNA analysis and microarray studies.

References

1. Allport DC, Gilbert DS, Outterside SM. MDI and TDI: safety, health and the environment: a source book and practical guide. New York: J. Wiley; 2003.
2. U.S. Environmental Protection Agency. Methylene diphenyl diisocyanate (MDI) and related compounds: action plan. 2019 [accessed 2019 Nov 5]. Available from: https://www.epa.gov/sites/production/files/2015-09/documents/mdi.pdf.
3. Jones K, Johnson PD, Baldwin PEJ, Coldwell M, Cooke J, Keen C, *et al*. Exposure to diisocyanates and their corresponding diamines in seven different workplaces. *Ann Work Expo Health* 2017;61:383–393.
4. Statista. Methylene diphenyl diisocyanate demand worldwide from 2011 to 2022t. 2018 [accessed 2018 Jan 5]. Available from: https://www.statista.com/statistics/750809/mdi-demand-worldwide/.
5. Fuchs S, Valade P. Clinical and experimental study of some cases of poisoning by desmodur T (1-2-4 and 1-2-6 di-isocyanates of toluene) [in French]. *Arch Mal Prof* 1951;12:191–196.
6. Bernstein DI. Genetics of occupational asthma. *Curr Opin Allergy Clin Immunol* 2011;11:86–89.
7. Redlich CA, Karol MH. Diisocyanate asthma: clinical aspects and immunopathogenesis. *Int Immunopharmacol* 2002;2:213–224.
8. Chan-Yeung M. Occupational asthma. *Chest* 1990;98:148S–161S.
9. Wisnewski AV, Jones M. Pro/Con debate: is occupational asthma induced by isocyanates an immunoglobulin E-mediated disease? *Clin Exp Allergy* 2010;40:1155–1162.
10. Bernstein DI, Cartier A, Côté J, Malo JL, Boulet LP, Wanner M, *et al*. Diisocyanate antigen-stimulated monocyte chemoattractant protein-1 synthesis has greater test efficiency than specific antibodies for identification of diisocyanate asthma. *Am J Respir Crit Care Med* 2002;166:445–450.
11. Liu Q, Wisnewski AV. Recent developments in diisocyanate asthma. *Ann Allergy Asthma Immunol* 2003;90:35–41.
12. Gledhill A, Wake A, Hext P, Leibold E, Shiotsuka R. Absorption, distribution, metabolism and excretion of an inhalation dose of [14C] 4,4′-methylenediphenyl diisocyanate in the male rat. *Xenobiotica* 2005;35:273–292.
13. Pauluhn J. Development of a respiratory sensitization/elicitation protocol of toluene diisocyanate (TDI) in Brown Norway rats to derive an elicitation-based occupational exposure level. *Toxicology* 2014;319:10–22.
14. Vanoirbeek JA, Tarkowski M, Ceuppens JL, Verbeken EK, Nemery B, Hoet PH. Respiratory response to toluene diisocyanate depends on prior frequency and concentration of dermal sensitization in mice. *Toxicol Sci* 2004;80:310–321.
15. Harkema JR, Morgan KT. Normal morphology of the nasal passages in laboratory rodents. In: Jones TC, Dungworth DL, Mohr U, editors. *Respiratory system*. Berlin, Heidelberg: Springer; 1996. pp. 3–17.
16. Kennedy AL, Singh G, Alarie Y, Brown WE. Autoradiographic analyses of guinea pig airway tissues following inhalation exposure to 14C-labeled methyl isocyanate. *Fundam Appl Toxicol* 1993;20:57–67.
17. Schroeter JD, Kimbell JS, Asgharian B, Tewksbury EW, Sochaski M, Foster ML, *et al*. Inhalation dosimetry of hexamethylene diisocyanate vapor in the rat and human respiratory tracts. *Inhal Toxicol* 2013;25:168–177.
18. Wisnewski AV, Liu J, Colangelo CM. Glutathione reaction products with a chemical allergen, methylene-diphenyl diisocyanate, stimulate alternative macrophage activation and eosinophilic airway inflammation. *Chem Res Toxicol* 2015;28:729–737.
19. Wisnewski AV, Liu J. Immunochemical detection of the occupational allergen, methylene diphenyl diisocyanate (MDI), *in situ*. *J Immunol Methods* 2016;429:60–65.

20. Sala-Rabanal M, Yurtsever Z, Berry KN, Nichols CG, Brett TJ. Modulation of TMEM16A channel activity by the von Willebrand factor type A (VWA) domain of the calcium-activated chloride channel regulator 1 (CLCA1). *J Biol Chem* 2017;292:9164–9174.
21. Tradtrantip L, Namkung W, Verkman AS. Crofelemer, an antisecretory antidiarrheal proanthocyanidin oligomer extracted from *Croton lechleri*, targets two distinct intestinal chloride channels. *Mol Pharmacol* 2010;77:69–78.
22. Jones K. Review of sangre de drago (*Croton lechleri*)--a South American tree sap in the treatment of diarrhea, inflammation, insect bites, viral infections, and wounds: traditional uses to clinical research. *J Altern Complement Med* 2003;9:877–896.
23. Castro JG, Chin-Beckford N. Crofelemer for the symptomatic relief of non-infectious diarrhea in adult patients with HIV/AIDS on anti-retroviral therapy. *Expert Rev Clin Pharmacol* 2015;8:683–690.
24. Wisnewski AV, Liu J, Nassar AF. LC-UV-MS and MS/MS characterize glutathione reactivity with different isomers (2,2′ and 2,4′ vs. 4,4′) of methylene diphenyl-diisocyanate. *EC Pharmacol Toxicol* 2019;7:205–219.
25. Wisnewski AV, Xu L, Robinson E, Liu J, Redlich CA, Herrick CA. Immune sensitization to methylene diphenyl diisocyanate (MDI) resulting from skin exposure: albumin as a carrier protein connecting skin exposure to subsequent respiratory responses. *J Occup Med Toxicol* 2011;6:6.
26. Council NR. *Guide for the care and use of laboratory animals*, 8th ed. Washington, DC: The National Academies Press; 2011.
27. Kleindl PA, Xiong J, Hewarathna A, Mozziconacci O, Nariya MK, Fisher AC, *et al*. The botanical drug substance crofelemer as a model system for comparative characterization of complex mixture drugs. *J Pharm Sci* 2017;106:3242–3256.
28. Macarthur RD, Hawkins TN, Brown SJ, Lamarca A, Clay PG, Barrett AC, *et al*. Efficacy and safety of crofelemer for noninfectious diarrhea in HIV-seropositive individuals (ADVENT trial): a randomized, double-blind, placebo-controlled, two-stage study. *HIV Clin Trials* 2013;14:261–273.
29. Stevens WW, Kim TS, Pujanauski LM, Hao X, Braciale TJ. Detection and quantitation of eosinophils in the murine respiratory tract by flow cytometry. *J Immunol Methods* 2007;327:63–74.
30. Keck W.M. Foundation Biotechnology Resource Laboratory. RN1easy total RNA isolation and cleanup protocol with optional DNase treatment. 2020 [accessed 2020 Apr 5]. Available from: https://medicine.yale.edu/keck/ycga/microarrays/protocols/RNeasyTotalRNAisolationandcleanupoptionalDNase_092508_21454_284_10813_v1.pdf.
31. Yale Center for Genome Analysis. Microarrays: Affymetrix GeneChip System. 2020 [accessed 2020 Apr 5]. Available from: https://medicine.yale.edu/keck/ycga/microarrays/affymetrix/.
32. Benjamini Y. Discovering the false discovery rate. *J R Stat Soc Series B Stat Methodol* 2010;72:405–416.
33. Jones MG, Floyd A, Nouri-Aria KT, Jacobson MR, Durham SR, Taylor AN, *et al*. Is occupational asthma to diisocyanates a non-IgE-mediated disease? *J Allergy Clin Immunol* 2006;117:663–669.
34. Kuperman DA, Lewis CC, Woodruff PG, Rodriguez MW, Yang YH, Dolganov GM, *et al*. Dissecting asthma using focused transgenic modeling and functional genomics. *J Allergy Clin Immunol* 2005;116:305–311.
35. Woodruff PG, Boushey HA, Dolganov GM, Barker CS, Yang YH, Donnelly S, *et al*. Genome-wide profiling identifies epithelial cell genes associated with asthma and with treatment response to corticosteroids. *Proc Natl Acad Sci USA* 2007;104:15858–15863.
36. Kamada F, Suzuki Y, Shao C, Tamari M, Hasegawa K, Hirota T, *et al*. Association of the hCLCA1 gene with childhood and adult asthma. *Genes Immun* 2004;5:540–547.
37. Nakanishi A, Morita S, Iwashita H, Sagiya Y, Ashida Y, Shirafuji H, *et al*. Role of gob-5 in mucus overproduction and airway hyperresponsiveness in asthma. *Proc Natl Acad Sci USA* 2001;98:5175–5180.
38. Zhu Z, Zheng T, Homer RJ, Kim YK, Chen NY, Cohn L, *et al*. Acidic mammalian chitinase in asthmatic Th2 inflammation and IL-13 pathway activation. *Science* 2004;304:1678–1682.
39. Orecchioni M, Ghosheh Y, Pramod AB, Ley K. Macrophage polarization: different gene signatures in m1(lps+) vs. Classically and m2(lps-) vs. Alternatively activated macrophages. *Front Immunol* 2019;10:1084.
40. Livak KJ, Schmittgen TD. Analysis of relative gene expression data using real-time quantitative PCR and the 2(-Delta Delta C(T)) Method. *Methods* 2001;25:402–408.
41. Wisnewski AV, Liu Q, Liu J, Redlich CA. Human innate immune responses to hexamethylene diisocyanate (HDI) and HDI-albumin conjugates. *Clin Exp Allergy* 2008;38:957–967.
42. Hoshino M, Morita S, Iwashita H, Sagiya Y, Nagi T, Nakanishi A, *et al*. Increased expression of the human $Ca2^{+}$-activated Cl- channel 1 (CaCC1) gene in the asthmatic airway. *Am J Respir Crit Care Med* 2002;165:1132–1136.
43. Brett TJ. CLCA1 and TMEM16A: the link towards a potential cure for airway diseases. *Expert Rev Respir Med* 2015;9:503–506.
44. Alevy YG, Patel AC, Romero AG, Patel DA, Tucker J, Roswit WT, *et al*. IL-13-induced airway mucus production is attenuated by MAPK13 inhibition. *J Clin Invest* 2012;122:4555–4568.
45. Bernstein JA. Overview of diisocyanate occupational asthma. *Toxicology* 1996;111:181–189.
46. Nakagami Y, Favoreto S Jr, Zhen G, Park S-W, Nguyenvu LT, Kuperman DA, *et al*. The epithelial anion transporter pendrin is induced by allergy and rhinovirus infection, regulates airway surface liquid, and increases airway reactivity and inflammation in an asthma model. *J Immunol* 2008;181:2203–2210.
47. Tarran R. Regulation of airway surface liquid volume and mucus transport by active ion transport. *Proc Am Thorac Soc* 2004;1:42–46.
48. Kondo M, Nakata J, Arai N, Izumo T, Tagaya E, Takeyama K, *et al*. Niflumic acid inhibits goblet cell degranulation in a Guinea pig asthma model. *Allergol Int* 2012;61:133–142.
49. Dasgupta P, Keegan AD. Contribution of alternatively activated macrophages to allergic lung inflammation: a tale of mice and men. *J Innate Immun* 2012;4:478–488.
50. Yucesoy B, Johnson VJ. Genetic variability in susceptibility to occupational respiratory sensitization. *J Allergy (Cairo)* 2011;2011:346719.